

On the emergence of flocking in birds

Adam Bauer*

May 9, 2021

Abstract

This essay will provide a brief overview of the many approaches scientists have taken to study bird flocking, including numerical, observational, and analytic methods. We discuss the pioneering work first done in numerical modeling and theoretical physics, and how these approaches are challenged by observational data. Lastly, we discuss an observationally motivated theoretical framework for studying flocking.

Contents

1	Introduction	1
2	Numerical models	1
3	Early theoretical model: the Vicsek model	2
3.1	Alterations to the Vicsek model	5
4	Observational data	5
5	Topological models of flocking	9
6	Summary	11

“... and the thousands of fishes moved as a huge beast, piercing the water. They appeared united, inexorably bound to a common fate. How comes this unity?” – Anonymous, 17th century [10]

*Department of Physics, University of Illinois Urbana-Champaign, 1110 W Green St Loomis Laboratory, Urbana, IL 61801

1 Introduction

The existence of collective behavior in nature has been the fascination of scholars for generations. Indeed, whether it was Ernst Ising modeling ordered magnetic systems or Friedrich Hayek considering “natural order” and its relation to law, the concepts of “order” and “disorder” consistently capture the attention of academics across disciplines. In particular, physicists and mathematicians have spearheaded the pursuit to analyze the existence and behavior of ordered structures in mathematical models of natural phenomena.

One such phenomena that has garnered considerable attention from both the physics and mathematics communities is flocking: the collective, synchronized movement of large collections of self-organizing agents. Flocking is ubiquitous in nature, and can be observed in organisms such as birds and sheep, as well as in schools of fish. Some flocking phenomena, such as starling murmurations, can consist of thousands of birds, all flying in unison [1]. In this essay, we will focus specifically on bird flocking, but the reader should remain aware that the material discussed herein is applicable to many of the examples given above.

Despite the commonplace nature of bird flocking, formulating a consistent model of flocking remains a difficult and interdisciplinary challenge for scientists. Indeed, until recently little observational data had been taken, making key model parameters difficult to estimate from field data. In the absence of data, computational scientists designed minimal models that reproduced flocking behavior in numerical experiments, marking the first step of progress towards understanding flocks [10]. Theoretical physicists also managed to make headway on developing models that predicted phase transitions within bird flocks [11]. However, a recent breakthrough observational study of bird flocking [2] led to the discovery of a topological interaction between birds, calling the assumptions of early numeric and theoretical models into serious question [1]. Since this study, models based on topological interactions have been formulated that reproduce flocking and predict the propagation of order throughout the flock with no free parameters [3].

In this essay, we intend to delve into the challenges in modeling bird flocking, as well as the progress made towards understanding emergent collective behavior in these systems. In §2, we will give an overview of the early numerical methods used to study bird flocking. In §3, we will discuss the first theoretical model of bird flocking and its associated phase transition. We will briefly touch on the modifications to this model in §3.1. In §4, we will discuss the observational record of bird flocking, and how recent observational studies have caused breakthroughs in our understanding of flocking. Lastly, we will discuss a new analytic theory of bird flocking in §5 which is based off of the topological interaction between birds discovered in [1]. We close with a summary in §6.

2 Numerical models

Given the lack of observational data on flocking, computational science was the first discipline to make real progress on studying the collective behavior of natural systems. The first computer model where emergent flocking was observed was developed by Reynolds, who endowed each independent particle moving along a three dimensional (3D) path with a distributed behavior model that led to collective flocking behavior [10]. Note that the “particles” within the simulation are meant to be interpreted as birds (called “bird-oids,” cutely nicknamed “boids” in the

paper). The behavioral model that dictated the behavior of each boids' local dynamics had the following tenants, listed in order of decreasing precedence:

1. Collision avoidance: avoid collisions with nearby flockmates;
2. Velocity matching: attempt to match velocity with nearby flockmates;
3. Flock centering: attempt to stay close to nearby flockmates. [10]

Simulations were initialized with random locations and velocities for all boids within a specified domain. After an initial “expansion burst,” where the rule of avoiding collisions dominated the system, flocks of boids developed by following the behavioral model laid out above, see Figure 1 for an example. Additionally, the flocks observed were “polarized,” in the sense that velocities were matched in both direction and speed, and were able to bifurcate around a static obstacle, as is observed in real flocks. In summary, simulated flocks demonstrate what the author describes as behavior “corresponding to the observer’s intuitive notion of what constitutes ‘flock-like motion’” [10].



Figure 1: The 3D animated flock of boids produced in [10]. The point of the boids indicates flight direction.

Models have built on the framework above to probe flocking at deeper levels. For example, in [8], Heppner and Grenander use a set of physically motivated nonlinear stochastic differential equations to model boids' flight paths, which resulted in flocking. In this set of equations, there existed terms that accounted for each of the rules listed above, as well as a term that accounted for the location of a roost (that attracted the flock) and some random Poisson noise, that was meant to simulate the impact of wind and other external perturbations. Strikingly, this model only produces flocking (over the roosting location) for *some set of parameters*; for other sets of parameters, no synchronized flock forms, and the group of boids resembles a “swarm of gnats” [8]. This suggests that flocking is a behavior that only exists for a certain set of parameter values, a concept we will revisit later in this report (see §3).

Reynolds, Heppner and Grenander all readily admit that while their simulations were successful, it is difficult to objectively verify how well the simulated flocks compare with flocks in nature [8, 10]. This reality raised the demand for observational data of flocks to compare with simulations. A similar problem was encountered in the theoretical community, discussed in the next section.

3 Early theoretical model: the Vicsek model

The Vicsek model (VM) is a first-of-its-kind numerical model of self-propelled agent based flocking put forth in 1995 [11]. The model consists of polar point particles on a 2D plane. These particles' motion is kept at constant velocity, and are allowed to move in any direction. The direction in which they move is updated at each timestep in the simulation by the average

velocity of other agents that are within its “domain of influence,” defined in this case as a sphere of unit radius around the particle. This model was shown to exhibit a phase transition, due to the spontaneous breaking of rotational symmetry.

Let us put the above into a mathematical framework. Consider N particles on a 2D plane with side length L . As discussed above, the i^{th} particle moves at constant speed \tilde{v} at an angle $\vartheta_i(t)$ with the x -axis. Therefore, at time $t + 1$, the particle position is given by

$$\vec{x}_i(t + 1) = \vec{x}_i(t) + \vec{v}_i(t)\Delta t, \quad (3.1)$$

where

$$\vec{v}_i(t) = \tilde{v}e^{i\vartheta_i(t)}, \quad (3.2)$$

is the velocity at time t . As we progress in time, \tilde{v} remains constant, but $\vartheta_i(t)$ must be updated to account for the influence of other agents. At the following timestep in the simulation, we therefore compute $\vartheta_i(t + 1)$ as

$$\vartheta_i(t + 1) = \langle \vartheta_i(t) \rangle_r + \delta\vartheta_i, \quad (3.3)$$

where $\langle \vartheta_i(t) \rangle_r$ is the average angle of travel for all particles within a radius r from particle i (including the i^{th} particle), and $\delta\vartheta_i$ is a random number chosen such that $-\eta/2 \leq \delta\vartheta_i \leq \eta/2$, where $\eta \in \mathbb{R}^+$ is an adjustable noise parameter. This is done to prevent against perfect alignment. Following the above prescription, VM has three free parameters: the density, $\rho = N/L^2$, the noise parameter, η , and \tilde{v} , the amount of distance covered by an agent in a timestep.

Simulations in [11] were carried out by fixing $\tilde{v} = 0.03$, and allowing η and ρ to vary. Initially a number of particles N were generated with random positions and directions. For low density and noise, the particles formed coherent small groups that moved in random directions. For high density and high noise the system was entirely randomly moving with very little correlation. When the density is large and the noise is small, the motion becomes ordered on a macroscopic scale and all agents tend to move in the same “spontaneously selected” direction [11]. See Figure 2 for examples of these cases, panels (b)–(d), respectively.

This spontaneous ordering signals a *phase transition* in the model from a disordered state (panels (a) – (c) of Figure 2) to an ordered state (Figure 2 panel (d)). To investigate this transition, Vicsek *et al.* define the average, normalized velocity v_a as

$$v_a := \frac{1}{N\tilde{v}} \left| \sum_{i=1}^N \vec{v}_i \right|. \quad (3.4)$$

Note if the system is entirely random, $v_a \rightarrow 0$, and if the system is completely coherent, $v_a \rightarrow 1$, thus making v_a an *order parameter*. Vicsek *et al.* find that for various values of the noise and density, the order parameter v_a behaves much like that of an order parameter of some equilibrium systems near the critical point, even though the system they consider is not in equilibrium. See Figure 2, panel (e) ((f), resp.) for the behavior of v_a with respect to η (ρ , resp.). They postulate this is because the agents are diffusing, which causes mixing, thus resulting in an effective long-range interaction radius [11].

Vicsek *et al.* derive a scaling law for the order parameter v_a in terms of the density and noise

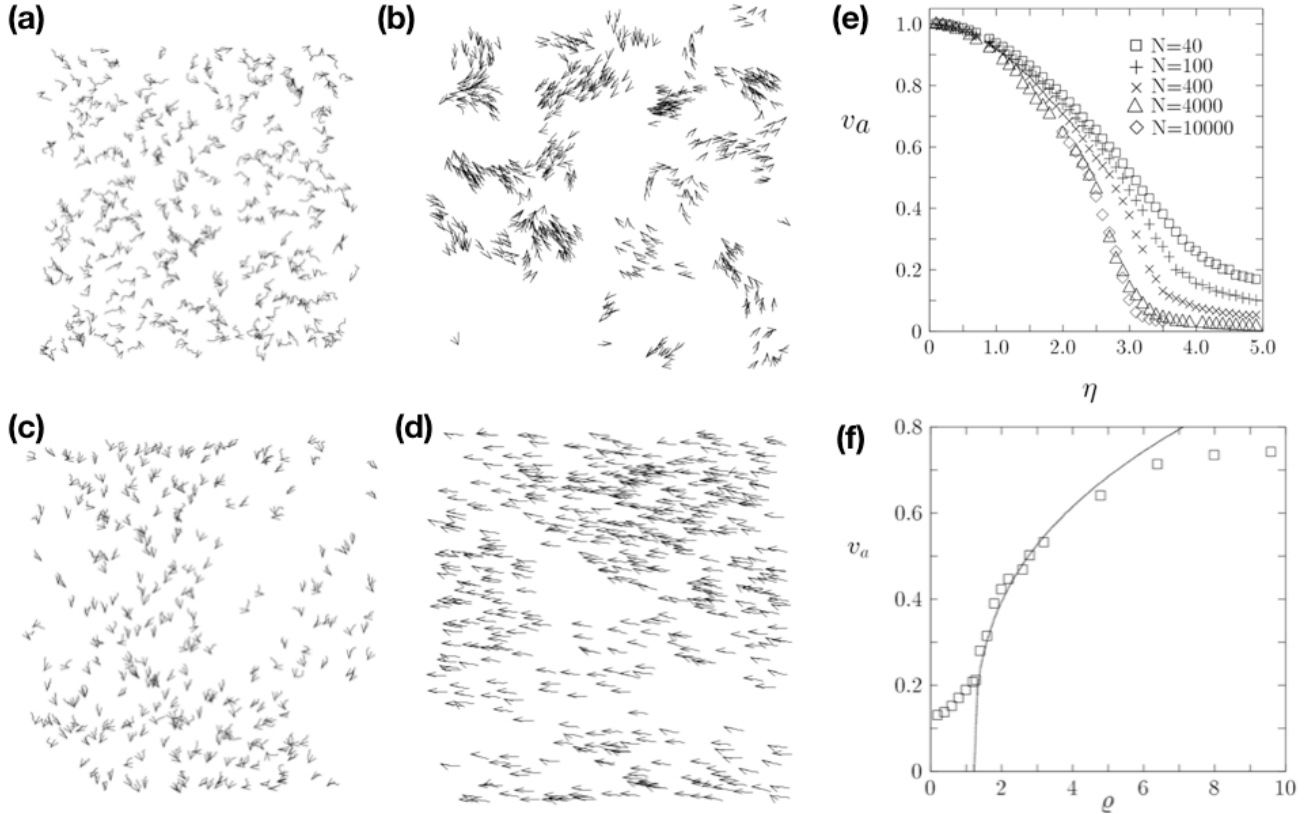


Figure 2: For panels (a) – (d), arrows indicate the agent direction of motion, and small curves show the agent location for the previous 20 timesteps. (a). Simulation results at $t = 0$. (b). Simulation results when density and noise are small. (c). Simulation results when density and noise is high. (d). Simulation results when density is high and noise is small; notice the macroscopic ordering in the system. (e). The order parameter v_a as a function of η for different particle numbers. (f). The order parameter v_a as a function of ρ . (Images taken from [11].)

in the thermodynamic limit ($L \rightarrow \infty$), such that

$$v_a \sim (\eta_c(\rho) - \eta)^\beta, \quad v_a \sim (\rho - \rho_c(\eta))^\delta, \quad (3.5)$$

where β, δ are the critical exponents and $\eta_c(\rho)$ and $\rho_c(\eta)$ are the critical noise and density in the thermodynamic limit, respectively. Vicsek *et al.* compute the critical exponents by regressing $\ln v_a$ against $\ln((\eta_c(L) - \eta)/\eta_c(L))$ and $\ln((\rho - \rho_c(L))/\rho_c(L))$ for some fixed values of ρ and η , respectively. They compute $\beta = 0.45 \pm 0.07$ and $\delta = 0.35 \pm 0.06$ [11]. As noted above, η_c depends on ρ , and Vicsek *et al.* predict the phase diagram for their model to be a line of critical η values, analogous to ferromagnets. This would indicate that the phase transition occurring in this model is of *second order* [11].

VM was the first successful model to predict a phase transition in self-propelled agent models. Since, VM has been built on, leading to new predictions. We discuss one such alteration in the next subsection.

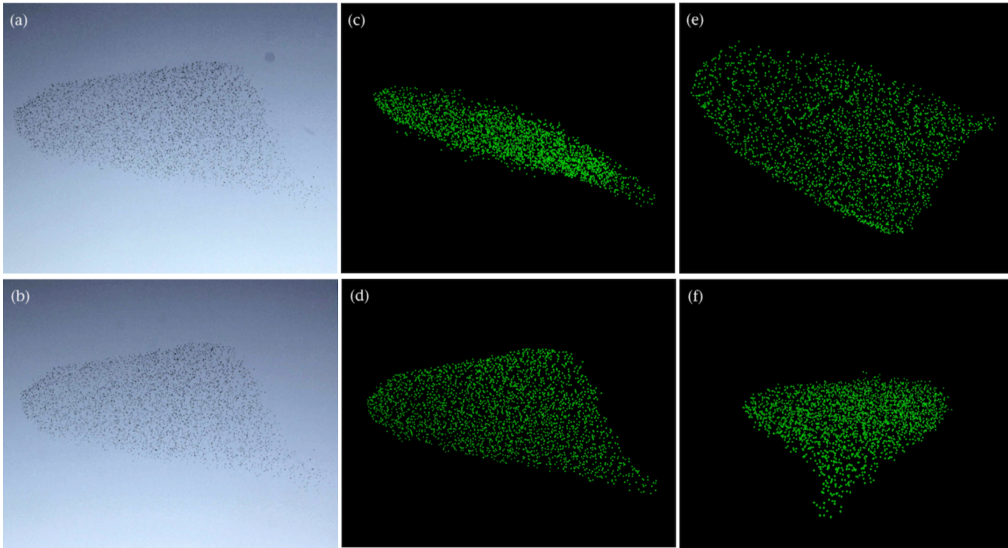


Figure 3: A typical flock and its 3D reconstruction. (a, b) Left-hand and right-hand, photos of the stereo pair, taken at the same time, but 25 m apart. (c,e,f) 3D reconstruction of the flock in the reference frame of the right-hand camera, under four different points of view. (d) Shows the reconstructed flock with the same perspective as (b). (Figure taken directly from [2].)

3.1 Alterations to the Vicsek model

One alteration made to VM in [6] was to limit the range of perception of each individual bird to a slice of a disk instead of a full disk, as was used in VM. This had a substantial impact on the result of the numerical simulation. The numerical studies done in [6] were carried out in the following way. They simulated the flight of N birds in 2D, as was done in VM, but with the average influence on ϑ_i only being averaged over a subset of a disk of radius r , such that (3.3) is changed such that

$$\vartheta_i(t+1) = \langle \vartheta_i(t) \rangle_{\Xi} + \delta\vartheta_i, \quad (3.6)$$

where $\Xi \subset \mathbb{R}^2$ is a subset of the unit disk. The size of Ξ was varied for each simulation and was parameterized by a “viewing angle,” that modeled the extent of a given bird’s visual perception. The same order parameter as in VM was studied here. Remarkably, the critical viewing angle for large system sizes was approximately $\phi_c \approx 0.2\pi$, or $\phi_c \approx 35^\circ$. This had a substantial impact on the result of the numerical simulation; in VM, the phase transition experienced in the model was of second order; in the modified case, the transition is first order.

However, just as was the case with early numerical models, VM and its alternatives were not motivated by any observational data, but rather by intuitive notions of biological interaction. As the theoretical and numerical study of flocking advanced, the demand for thorough observational investigation grew; this demand was eventually met by Ballerini and her collaborators in 2007, finally presenting an opportunity for theory to be checked by real-world observations.

4 Observational data

Although bird flocking is readily observable with our eyes, capturing the behavior on scientific instruments has been a consistent challenge. Field observations, prior to 2007, suffered from

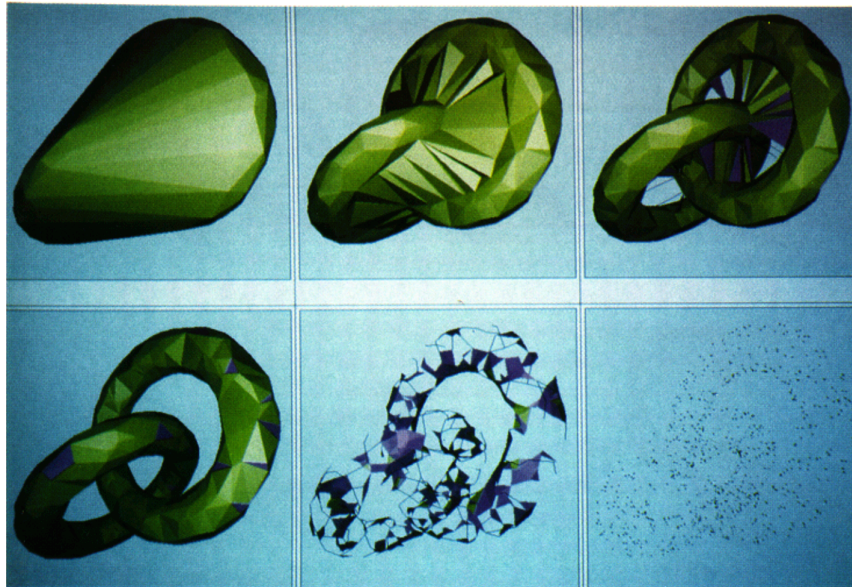


Figure 4: Shown is the shape derived using the α -parameter algorithm for a random set of points generated on the surface of two linked tori. The top left image is meant to be interpreted as $\alpha \rightarrow \infty$, whereas the bottom right is for $\alpha = 0$. Notice for some critical value of α , the shape of the two individual tori is nearly resolved. (Figure taken directly from [7].)

two main limitations: the number of individuals observed is small (i.e., tens of birds) and the group arrangements were loose, in direct opposition to the highly cohesive formations we wish to study (see [9] for an example of a field study incorrectly concluding that flocks are loosely assembled due to these limitations) [2]. An additional hurdle for field scientists is that numerous images, from multiple different angles, are needed in order to reconstruct the three dimensional formation of the flock from two dimensional pictures.

These complications were overcome for the first time in 2007 by Ballerini *et al.*, who use statistical physics, optimization theory and computer vision techniques to resolve their set of two dimensional images into full three dimensional images of bird flocks [2]. To accomplish this, Ballerini *et al.* used a trifocal technique, combined with image reconstruction algorithms described in [4]; an example of one of the three dimensional reconstructions is shown in Figure 3. After taking three months of observational data, Ballerini *et al.* were able to gather data on approximately 500 flocking events, of which 10 were able to be fully analyzed due to software constraints and photographic resolution restrictions. In all of the flocks analyzed, the number of birds never sank beneath 400, and never exceeded 8000 [2].

The results in [2] are obtained using an impressive suite of image software discussed in [4]. A summary of their methodology is as follows. Consider an image; after processing, the end result is a finite set of points, $\Sigma \subset \mathbb{R}^3$, where each imaged bird is located by an element of Σ . Using this set of points, Ballerini *et al.* employ an α -shape algorithm to find the border of the flock; this is equivalent to computing the “shape” of the flock. This algorithm derives a well-defined polytope from the Delaunay triangulation of Σ , with the level of resolution mediated by $\alpha \in \mathbb{R}$ [7]. Note that Delaunay triangulation is a method commonly employed in computational science that, for a cloud of discrete points Σ , derives a triangulation $DT(\Sigma)$, such that no point of Σ is inside the circumcircle of a triangle in $DT(\Sigma)$ [5]. See Figure 4 for an example of the impact that varying α has on the resulting shape of the point cloud.

Once the border was defined, the volume of the flock was computed using the Delaunay triangulation, only considering birds internal to the border. The dimensions of the flock were derived in the following way. The thickness, I_1 , was defined as the diameter of the largest sphere contained within the flock’s boundary. Exploiting the fact that the thickness is the shortest dimension of the flock by construction (see panel (c) of Figure 3), a plane was fitted to the flock, with the axis orthogonal to the plane being labeled as \vec{I}_1 . The second dimension I_2 was defined as the diameter of the smallest circle contained in the 2D projection of the flock onto the plane; the 2D projection was then fit to a line, which defined the third dimension \vec{I}_3 . The axis \vec{I}_2 was then found by completing the 3D orthogonal basis containing the other axes \vec{I}_1 and \vec{I}_3 [2].

The main results from their analysis is the following. Ballerini *et al.* measured the aspect ratios of the flock with respect to the thickness I_1 , i.e., the quantities I_2/I_1 and I_3/I_1 . The average over all events was found to be $I_2/I_1 = 2.8 \pm 0.4$ and $I_3/I_1 = 5.6 \pm 1.0$, where they report 95% confidence intervals [2]. These results confirm what was visually represented in Figure 3 panel (c), that flocks are generally thin in one dimension and prefer to spread out laterally. This finding is supported by their analysis on the orientation of the flock. Defining \vec{g} as the unit vector pointing in the direction of gravity and \vec{v} as the unit vector pointing in the direction of the flock’s center of mass velocity, Ballerini *et al.* find that, on average, $|\vec{I}_1 \cdot \vec{g}| = 0.93 \pm 0.04$, whereas $|\vec{v} \cdot \vec{g}| = 0.13 \pm 0.05$ and $|\vec{v} \cdot \vec{I}_1| = 0.19 \pm 0.08$ [2]. The conclusion we can draw from these findings is that flocks tend to align their thinnest dimension along the vertical axis (i.e., parallel to gravity), and as a unit move parallel to the Earth’s surface. This can easily be explained via energetic considerations; there is a higher energy cost to oppose gravity and fly in the vertical direction, therefore it is more energetically favorable for the flock to fly parallel to the ground. Also, this supports the assumption that 2D models can accurately reproduce realistic flocking behavior, as was done in [11, 6].

Another important result is that the density of flocks varied substantially, and did not depend on the number of birds belonging to the flock [2]. Furthermore, the nearest neighbor distance also did not depend on the size of the group, which is contrary to patterns observed in fish schools and in numerical simulations. This result was analyzed further by Ballerini and her collaborators in [1], where they found that the interaction between birds does *not* depend on metric distance (as most models assume¹), but on the *topological distance*. This implies a stunning conclusion: the “attraction” between two birds depends on the number of individual birds that separate them, rather than the physical distance away; so long as there are no birds in between a pair of birds, it matters not whether they are separated by 1 m or 10 m. Ballerini *et al.* reports that on average, individual birds interact with about six to seven of their nearest neighbors [1].

The methodology used in [1] to reach this conclusion is as follows. For each bird in an imaged flock, Ballerini *et al.* measure the angular orientation of its nearest neighbor with respect to the flock’s direction of motion, i.e., the neighbor’s bearing and elevation. This is done for both the nearest neighbor and the tenth closest bird to the reference bird; see Figure 5. The results in Figure 5 are derived by assigning a unit vector \vec{u}_i for the i^{th} bird in the direction of its nearest neighbor. Each unit vector is placed at the origin, and the density normalized by the isotropic case is plotted on the unitary sphere. Ballerini *et al.* note that this anisotropic pattern continues if one plots the second nearest neighbor, but is weaker, and continues to decay as we venture away from the reference bird.

¹The numerical simulations discussed in §2 and models discussed in §3 did not restrict the number of neighbors any one agent could interact with within some “neighborhood” around the agent. Furthermore, there was no *a priori* justification for the size of the local neighborhood assumed in the models.

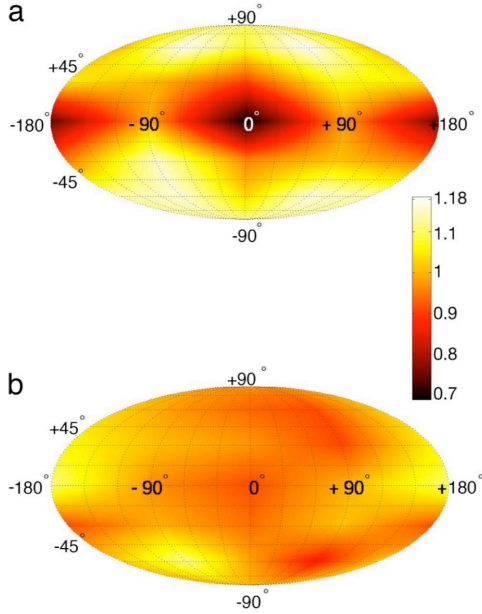


Figure 5: Shown is the angular distribution of nearest neighbors. Note the elevation $\phi \in [-90^\circ, 90^\circ]$ is the vertical direction and the bearing $\alpha \in [-180^\circ, 180^\circ]$ is on the horizontal axis. In this projection, $\alpha = 0^\circ, \phi = 0^\circ$ is the front of the bird, whereas $\alpha = \pm 180^\circ, \phi = 0^\circ$ is the rear of the bird. The group velocity \vec{v} goes through the center of the map, i.e., into the page. (Top). Shown is the angular distribution of the first nearest neighbor. Note the strong anisotropy in front and in the rear of birds. (Bottom). Shown is the angular distribution of the tenth nearest bird. This closely resembles a random distribution of points. (Figure taken from [1].)

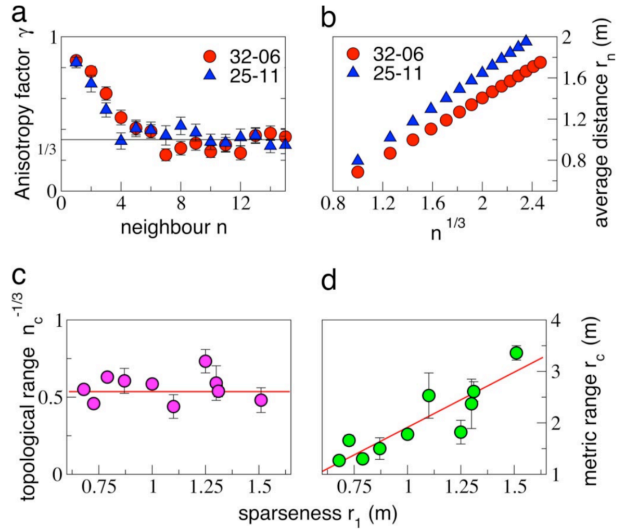


Figure 6: (a). Shown is the average value of $\gamma(n)$ for the 15 nearest neighbors of each bird in two different flocks. (b). The average distance r_n of the n^{th} nearest neighbor plotted against $n^{1/3}$; this gives a measure of sparseness. The slope of the line is proportional to r_1 . (c). Topological range n_c plotted against r_1 . Notice the lack of correlation. (d). Metric range r_c plotted against r_1 . A very clear linear relation is observed. (Figure taken from [1].)

To quantify this anisotropy, Ballerini *et al.* compute a function $\gamma(n)$, where n is the number of nearest neighbor birds away from the reference bird we are considering. Note that $\gamma \rightarrow 1/3$ is the isotropic case, and $\gamma > 1/3$ if the distribution is anisotropic; i.e., panel (a) of Figure 5 would have a value such that $\gamma(1) > 1/3$. The average value of $\gamma(n)$ is computed and shown in panel (a) of Figure 6 for the 15 nearest birds to each bird in the flock, for two sets of observational data. The result is clear: the angular distribution becomes isotropic around 5-8 birds away from the reference bird, on average. We denote this critical number of birds as n_c . This result, however, is not sufficient to conclude that the interaction between birds is dictated by topology rather than metric distance; indeed, the first nearest bird to a reference bird can be described by $n = 1$, but also by a distance r_1 away from the bird. These quantities are related by the density of the flock. Thus, one may also consider the average distance the n^{th} bird is away from the reference bird; we call this quantity r_c in what follows.

As noted in [2], the density varied drastically between flocks. Therefore, n_c and r_c cannot

remain constant for every set of data; if the interaction between birds is truly dependent on metric distance, r_c is constant, and therefore in a small density flock, n_c would be small, since less birds would be inside a given reference bird’s “domain of influence.” Conversely, if the interaction between birds is dependent on topological distance n_c , then for a low density flock, r_c should get large, as birds farther away in metric distance from a given reference bird will still influence the reference bird. The inverse of the above statements is true for high density flocks.

To determine whether it is the metric or topological distance that dictates the interaction between birds, Ballerini *et al.* compute n_c and r_c as functions of density [1]. To do this in a quantitative way, Ballerini *et al.* note that the amount of birds inside a ball of radius r is given by $n^{1/3} \sim r/r_1$, where r_1 is the average distance between a reference bird and its first nearest neighbor, which can be inferred from the data, see Figure 6(b). The critical relations are given by the same equation, *i.e.*, $n_c^{1/3} \sim r_c/r_1$. In the metric distance scenario, r_c is constant, and thus we expect a linear relationship between $n_c^{-1/3} \sim r_1$. On the other hand, in the topological scenario, n_c is constant, and so we expect that $r_1 \sim r_c$, see Figure 6(c) and (d) for results. It is found that there is no significant correlation between $n_c^{-1/3}$ and r_1 , but there is significant correlation between r_1 and r_c , thus strongly supporting the argument that the underlying interaction in bird flocking is topological, not dictated by metric distance [1].

Ballerini *et al.* further support this hypothesis via numerical experiments. They note that, in field observations of flocking, flocking behavior is *robust*, often not splitting into more than 2 or 3 separate units under perturbations [1, 2]. They therefore simulate both the Vicsek model [11] in the parameter range where flocking occurs and an alternative Vicsek model, where the interaction is topological rather than metric, under a perturbation meant to model a predator. After Monte Carlo simulation over numerous parameter values, the probability that the flock is broken up into a number of units M is displayed by Figure 7. Clearly, Ballerini *et al.* conclude, topological interactions are more stable under perturbations than metric distance based models, further supporting their findings from data analysis. In the next section, we discuss a model that involve topological interactions, as supported by the above considerations.

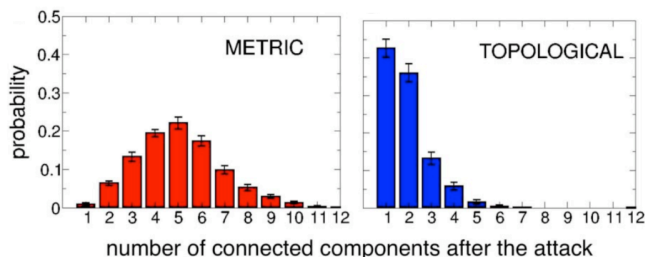


Figure 7: Shown is the probability distribution of the number of connected components of a flock after being subjected to a perturbation modeled after a predator. (Figure taken from [1].)

5 Topological models of flocking

In 2012, a model put forth by Bialek *et al.* was formulated to agree with the observational findings in [1, 2] that relied on no modeling assumptions; it relies only on the principle of maximum entropy [3]. The model is constructed as follows. Consider a flock of N birds. To each bird, we attach a velocity \vec{v}_i , which is normalized such that $\vec{s}_i := \vec{v}_i/|\vec{v}_i|$. Bialek *et al.* follow the hypothesis that flocks admit stationary states, which implies that the velocities \vec{s}_i can be drawn from a probability distribution $P(\{\vec{s}_i\})$. However, they cannot infer $P(\{\vec{s}_i\})$ from experimental data; instead, they infer the matrix of correlations between normalized velocities

$C_{ij} := \langle \vec{s}_i \cdot \vec{s}_j \rangle$. They then choose the probability distribution $P(\{\vec{s}_i\})$ that is as random as it can be while still matching experimental data, i.e., the distribution with maximum entropy [3]. The probability distribution is therefore given by

$$P(\{\vec{s}_i\}) = \frac{1}{Z(\{J_{ij}\})} \exp\left(\frac{1}{2} \sum_{i=1}^N \sum_{j=1}^N J_{ij} \vec{s}_i \cdot \vec{s}_j\right), \quad (5.1)$$

where $Z(\{J_{ij}\})$ is the partition function and J_{ij} is the interaction strength that corresponds to C_{ij} . Bialek *et al.* use

$$\langle \vec{s}_i \cdot \vec{s}_j \rangle_P = \langle \vec{s}_i \cdot \vec{s}_j \rangle_{\text{experiment}}, \quad (5.2)$$

to match J_{ij} to the experimentally determined C_{ij} . It is interesting to note that the model put forth by (5.1) is exactly equivalent to the Heisenberg model of magnetic systems, with $k_B T = 1$. As in most physical systems, once the Hamiltonian is determined, Langevin dynamics describe the plausible dynamics of relaxing towards equilibrium, given by

$$\frac{d\vec{s}_i}{dt} = -\frac{\partial H}{\partial \vec{s}_i} + \vec{\eta}_i(t) = \sum_{j=1}^N J_{ij} \vec{s}_j + \vec{\eta}_i(t), \quad (5.3)$$

where $\vec{\eta}_i(t)$ is a white noise term. Finding trajectories that solve (5.3) produces trajectories that are drawn from (5.1) [3].

Bialek *et al.* incorporate the findings of [1, 2] by allowing the interaction strength to be independent of the bird's identity, which sets the interaction strength $J > 0$ to a constant, and allowing a given bird to only interact with its n_c nearest neighbors. This simplifies (5.1) to

$$P(\{\vec{s}_i\}) = \frac{1}{Z(J, n_c)} \exp\left(\frac{J}{2} \sum_{i=1}^N \sum_{j \in n_c^i} \vec{s}_i \cdot \vec{s}_j\right), \quad (5.4)$$

where $j \in n_c^i$ means that bird j belongs to the set of nearest neighbors for bird i . Note this simplification also simplifies the calculation of the correlation, which also becomes a constant, and is given by

$$C_{int} = \frac{1}{N} \sum_{i=1}^N \frac{1}{n_c} \sum_{j \in n_c^i} \langle \vec{s}_i \cdot \vec{s}_j \rangle \approx \frac{1}{N} \sum_{i=1}^N \frac{1}{n_c} \sum_{j \in n_c^i} \vec{s}_i \cdot \vec{s}_j. \quad (5.5)$$

A summary of the results found in [3] is as follows. First, they compute the correlation C_{int} predicted by the model via equation (5.5) as a function of J and compare it to the experimental value of correlation, see Figure 8(a); using $C_{int}(J, n_c) = C_{int}^{exp}$, they determine $J(n_c)$. Using probability data as a function of n_c , they fix n_c as the value where the log likelihood is maximized; this then fixes n_c and J in the maximum entropy state, see Figure 8(b). This procedure is repeated for all flocks, and the mean and standard deviation is computed over time.

In Figure 8(c) and (d), the values of J and n_c are computed as a function of the flock's spatial size, L , respectively. Note that [3] do not report any trend in the values of J or n_c as a function of the flock size. The result for n_c agrees with the findings of [1]; since n_c is constant, it does not matter whether a pair of birds are separated by 1 m or 5 m, so long as they are sufficiently close to each other in topological distance.

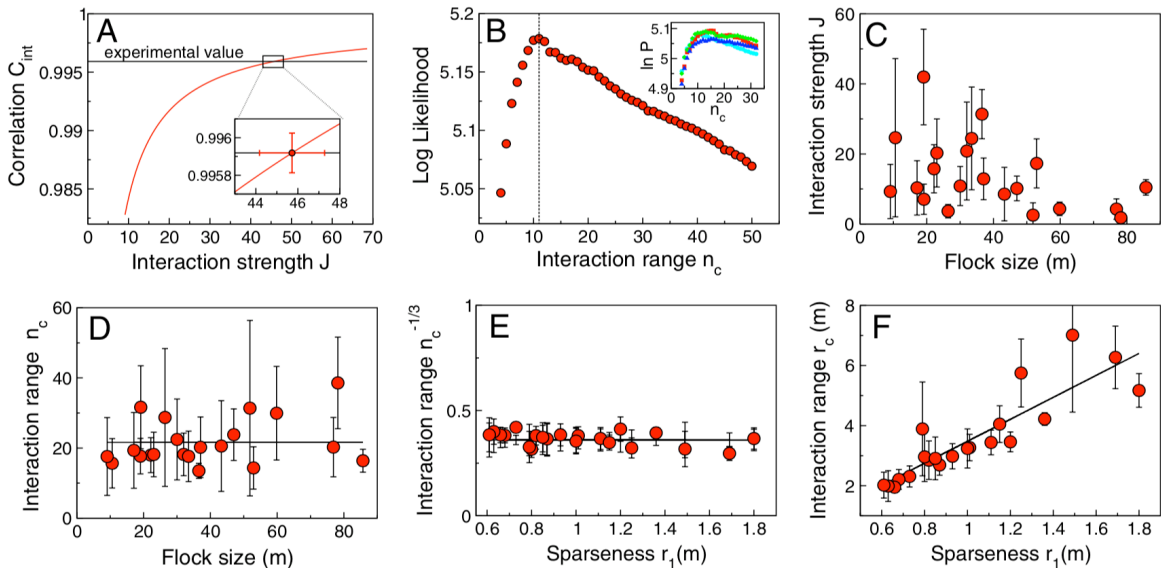


Figure 8: (a). Estimation of C_{int} as a function of J with $n_c = 11$. (b). The log-likelihood of the data per bird ($\langle P(\{\vec{s}_i\}) \rangle_{\text{exp}}/N$) as a function of n_c with J optimized for each n_c . Maximum is at $n_c \approx 11$. (c). Inferred value of J as a function of flock size, averaged over all snapshots of the same flock. (d). As in (c), but for n_c . (e). Inferred value of the topological range $n_c^{-1/3}$ against sparseness r_1 . (f). As in (e), but for metric range r_c . (Figure taken from [3].)

The last two panels of Figure 8, panels (e) and (f), test the same hypothesis as [1] involving correlations between n_c , r_1 , and r_c , where r_1 is the sparseness and r_c is the critical metric distance of a given bird’s “domain of influence,” see §4 for a detailed overview of the arguments. In short, [3] finds no linear correlation between $n_c^{-1/3} \sim r_1$, yet finds significant linear correlation between $r_c \sim r_1$, thus affirming the hypothesis that the interactions in bird flocks are determined by topological distance rather than metric distance.

The results presented in [3] agree well with those found in [1], however, Bialek *et al.* overestimate the topological interaction distance n_c by about 5 birds compared to [1]. Even with this numerical difference, qualitatively, the model proposed in [3] predicts the propagation of directional order throughout the flock with no tunable free parameters. Additionally, it predicts long range, scale free correlations between pairs of birds, as well as local effects. It is emphasized again that this model is formulated on a fundamentally different set of axioms than what was used to postulate the models in §2 and §3, and reproduces similar flocking behavior using the general principle of entropy maximization. Furthermore, the axioms of Bialek *et al.* are well motivated by observations [1, 2], making this theory promising for future investigation into the nature of bird flocking.

6 Summary

In this work, we present the myriad of ways that scientists have investigated bird flocking across disciplines. In computational science, we discussed how the first numerical simulations of bird flocking were carried out, and the set of rules enforced on the simulated agents. We similarly discussed early theoretical models, namely the Vicsek model of flocking, and its framework for studying flocking, including the discovery of a phase transition. Recent alterations made to the

Vicsek models find the type of phase transition occurring within the model changes if you limit the amount of information a given bird perceives from its environment. The weakness of the above approaches is that their assumptions, while intuitive, are not supported by observational data. We then summarize the findings of observational studies, and how these studies challenged the assumptions of the Vicsek model and early numerical models. Finally, we close with an exploration of an updated model of bird flocking, containing no free parameters, that is based off of observational data. This model is found to agree well with the data used in the aforementioned observational study.

References

- [1] M. Ballerini, N. Cabibbo, R. Candelier, A. Cavagna, E. Cisbani, I. Giardina, V. Lecomte, A. Orlandi, G. Parisi, A. Procaccini, M. Viale, and V. Zdravkovic. Interaction ruling animal collective behavior depends on topological rather than metric distance: Evidence from a field study. *Proceedings of the National Academy of Sciences*, 105(4):1232–1237, 2008.
- [2] M. Ballerini, N. Cabibbo, R. Candelier, A. Cavagna, E. Cisbani, I. Giardina, A. Orlandi, G. Parisi, A. Procaccini, M. Viale, and V. Zdravkovic. Empirical investigation of starling flocks: a benchmark study in collective animal behaviour. *Animal Behaviour*, 76(1):201–215, 2008.
- [3] W. Bialek, A. Cavagna, I. Giardina, T. Mora, E. Silvestri, M. Viale, and A. M. Walczak. Statistical mechanics for natural flocks of birds. *Proceedings of the National Academy of Sciences*, 109(13):4786–4791, 2012.
- [4] A. Cavagna, I. Giardina, A. Orlandi, G. Parisi, A. Procaccini, M. Viale, and V. Zdravkovic. The starflag handbook on collective animal behaviour: Part i, empirical methods, 2008.
- [5] J. A. De Loera, J. Rambau, and F. Santos. *Triangulations: Structures for Algorithms and Applications*. Springer Publishing Company, Incorporated, 1st edition, 2010.
- [6] M. Durve and A. Sayeed. First-order phase transition in a model of self-propelled particles with variable angular range of interaction. *Phys. Rev. E*, 93:052115, May 2016.
- [7] H. Edelsbrunner and E. P. Mücke. Three-dimensional alpha shapes. *ACM Trans. Graph.*, 13(1):4372, Jan. 1994.
- [8] F. Heppner and U. Grenander. Ubiquity of chaos, chapter a stochastic nonlinear model for coordinated bird flocks. *The Ubiquity of Chaos, Chapter A Stochastic Nonlinear Model for Coordinated Bird Flocks*, pages 233–238, 01 1990.
- [9] R. Miller and W. J. Stephen. Spatial relationships in flocks of sandhill cranes (*grus canadensis*). *Ecology*, 47:323–327, 1966.
- [10] C. W. Reynolds. Flocks, herds and schools: A distributed behavioral model. *SIGGRAPH Comput. Graph.*, 21(4):2534, Aug. 1987.
- [11] T. Vicsek, A. Czirak, E. Ben-Jacob, I. Cohen, and O. Shochet. Novel type of phase transition in a system of self-driven particles. *Physical Review Letters*, 75(6):12261229, Aug 1995.